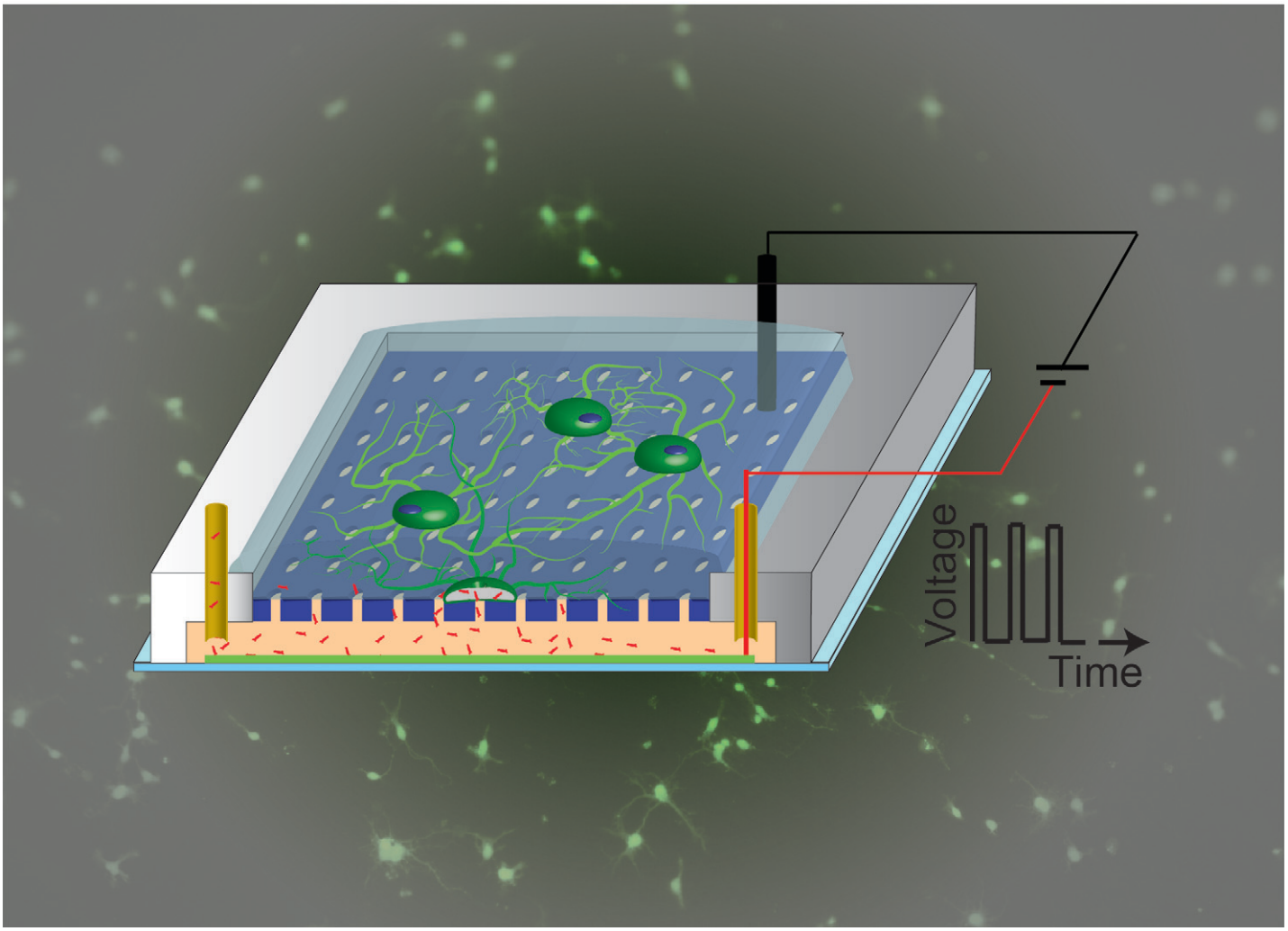

Featuring work done by Prof. Horacio D. Espinosa and Prof. John A. Kessler at Northwestern University, USA.

Title: Microfluidic device for stem cell differentiation and localized electroporation of postmitotic neurons

A simple, yet robust method for long-term on-chip cell culture and transfection of sensitive adherent cells was developed utilizing unique advantages of microfluidics systems. The capabilities of the localized electroporation device (LEPD) were demonstrated by supporting neural stem cells during differentiation and delivering green fluorescent protein plasmids into neurons while maintaining cell viability.

As featured in:

See Horacio D. Espinosa *et al.*, *Lab Chip*, 2014, **14**, 4486.

ROYAL SOCIETY OF CHEMISTRY

www.rsc.org/loc

Registered charity number: 207890

Lab on a Chip

PAPER

View Article Online
View Journal | View Issue

Cite this: *Lab Chip*, 2014, **14**, 4486

Microfluidic device for stem cell differentiation and localized electroporation of postmitotic neurons†

Wonmo Kang,[ab] Juan P. Giraldo-Vela,[b] S. Shiva P. Nathamgari,[a] Tammy McGuire,[c] Rebecca L. McNaughton,[ab] John A. Kessler[c] and Horacio D. Espinosa*[a]

Received 19th June 2014,
Accepted 26th August 2014

DOI: 10.1039/c4lc00721b

www.rsc.org/loc

New techniques to deliver nucleic acids and other molecules for gene editing and gene expression profiling, which can be performed with minimal perturbation to cell growth or differentiation, are essential for advancing biological research. Studying cells in their natural state, with temporal control, is particularly important for primary cells that are derived by differentiation from stem cells and are adherent, *e.g.*, neurons. Existing high-throughput transfection methods either require cells to be in suspension or are highly toxic and limited to a single transfection per experiment. Here we present a microfluidic device that couples on-chip culture of adherent cells and transfection by localized electroporation. Integrated microchannels allow long-term cell culture on the device and repeated temporal transfection. The microfluidic device was validated by first performing electroporation of HeLa and HT1080 cells, with transfection efficiencies of ~95% for propidium iodide and up to 50% for plasmids. Application to primary cells was demonstrated by on-chip differentiation of neural stem cells and transfection of postmitotic neurons with a green fluorescent protein plasmid.

Introduction

Transfection of nucleic acids and other molecules into cultured cells is a widely used method to study gene function and disease mechanisms.[1–6] However, traditional transfection tools are not suitable for the development of a comprehensive technique for cell derivation, cloning, and functional assessment that is needed to advance research toward a more biologically relevant experimental environment. Indeed, traditional transfection methods usually require cell suspension, which may perturb cellular pathways under investigation, and are often extremely harsh for sensitive primary cells. These disadvantages are particularly problematic for studying adherent primary cells such as neurons, where transfection of adherent cells is needed to explore the pathogenic mechanisms of neural diseases and to develop gene therapies for disorders such as Alzheimer's, Parkinson's, epilepsy, and many others.[7–9]

Current methods for neural studies include transfection by viruses,[9–11] microinjection,[12,13] bulk electroporation,[14–19] microfluidic electroporation[20–24] and single-cell electroporation.[25–27] These methods are often limited by either achieving high transfection efficiency at the cost of cell health or having low throughput when temporal control is important. These tradeoffs create significant challenges for studying differentiated mammalian neurons because they are very sensitive to physical stress, alterations in temperature, pH shifts, and changes in osmolarity. Indeed, current methods for transfection of postmitotic neurons have been described as labor-intensive, inefficient, unreliable, and/or cytotoxic.[28] More recently, nanowire-based transfection methods[14,29,30] have been successfully demonstrated for high throughput transfection of cell lines, however, understanding the effect of the nanowire substrate on cellular pathways and phenotype control is still in its infancy. Slow growth of cells, development of irregular cell contours, and lipid scrambling have been observed.[31,32]

Electroporation-based transfection methods have become popular as they offer the highest transfection efficiency among non-viral methods. Electroporation relies on the creation of transient and reversible nanopores in the cell membrane by application of an external electric field.[33,34] However, bulk electroporation methods, including nucleofection[35] (modified electroporation) and microporation, suffer from significant disadvantages: i) the entire cell population is exposed to very

[a] *Department of Mechanical Engineering, Northwestern University, Evanston, IL 60208, USA. E-mail: espinosa@northwestern.edu; Fax: +1 847 491 3915; Tel: +1 847 467 5989*
[b] *iNfinitesimal LLC, Skokie, IL 60077, USA*
[c] *Department of Neurology, Northwestern University, Chicago, IL 60611, USA*
† Electronic supplementary information (ESI) available. See DOI: 10.1039/c4lc00721b

high voltages, which routinely causes cell death rates of up to 50%, and/or ii) cells need to be suspended during the process. To address these disadvantages while still utilizing electroporation, the Espinosa group developed nanofountain probe electroporation (NFP-E) for single-cell transfection of adherent cells with cell selectivity, dosage control, and high transfection efficiency and viability.[36,37] This method uses a microfluidic cantilever to apply a localized electric field to an adherent cell for transfection. Here we extend the localized electroporation technique, utilizing the advantages of micro/nano systems, to develop a microfluidic device for long-term on-chip cell culture and temporal transfection.

Our goal was to develop a novel microfluidic device to (1) optimally culture cells during differentiation and/or expansion, (2) efficiently deliver molecules into these adherent cells by localized electroporation, and (3) minimize external stress during transfection to achieve high viability. The microfluidic device presented here achieved these goals, and although the main application presented here involves transfection of neurons, the device is a general tool that can be used for culture and transfection of any adherent cells of interest. To demonstrate this point and to define the electroporation protocols, we first present experimental results using HeLa and HT1080 cells and then demonstrate transfection of mature neurons derived from mice neurospheres.

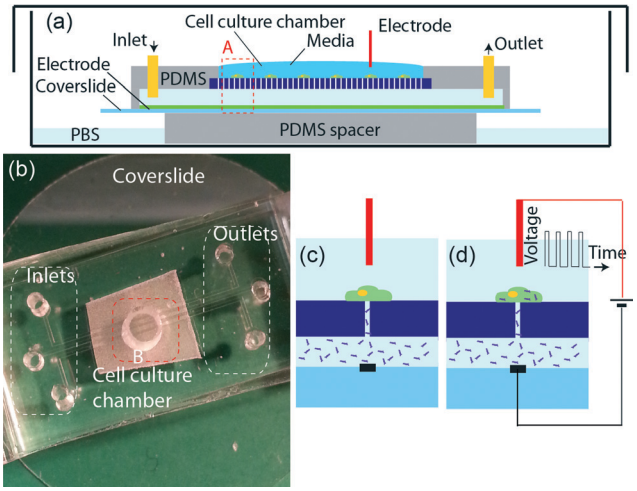

Fig. 1 (a) A schematic of the LEPD enclosed within a Petri dish to maintain humidity for long term cell culture, (b) an optical image of the LEPD, made of PDMS, with three inlets and three outlets connected to microchannels, and (c) and (d) magnified views of area A in the schematic drawing depicting an adhered cell covering a micropore, and the mechanism of delivery of molecules by localized electroporation, respectively.

Results and discussion

Device design

We designed a novel microfluidic device that can flow cells into a microwell, allow cells to adhere, and transfect them by means of localized electroporation. Localized transmembrane voltages are less likely to cause cell damage or death while increasing transfection efficiency. Using built-in microchannels, cell culture media can be continuously fed to cells, in a cell culture chamber, without directly exposing such cells to the fluid flow. This enables automated long-term cell culture for sensitive cells and prevents application of shear stresses, which could induce cell damage or phenotypic changes.[38–40] In addition, numerous solutions with different molecules can be delivered to the cells at different times, allowing for high-throughput temporal transfection without the need for cell re-suspension.

We used polydimethylsiloxane (PDMS) because it is commonly used for rapid prototyping of microfluidic devices; however, if intrinsically fluorescent solutions are fed into the microchannels, the fluorescent molecules may be absorbed into the PDMS matrix and introduce undesired background noise during fluorescence imaging. To prevent or minimize such absorption, the microchannels can be chemically treated to passivate the PDMS surfaces[41,42] with Pluronic F-127 (see ESI† Fig. S1).

The design of the on-chip localized electroporation device (LEPD) is shown in Fig. 1. It consists of microchannels, a cell culture chamber, built-in electrodes, and a porous substrate containing micro- or nanochannels. The cell culture chamber is 3 mm in diameter, and the width and height of the microchannels are 200 μm and ~20 μm, respectively. One electrode is built-in on a fabricated glass cover slide while the other Ag/AgCl wire electrode is submerged into the media in the cell culture chamber. The two electrodes are separated by a perforated substrate on which cells are plated. On-chip cell culture is maintained by continuous flow of culture media through the circulation microchannels (Fig. 1a) located beneath the perforated substrate. For intercellular delivery by electroporation, a solution containing biomolecules to be delivered into the cells is loaded into the circulation microchannels, as shown schematically in Fig. 1c. A voltage is applied between the two microelectrodes to trigger formation of nanopores on the cell membrane, Fig. 1d. The molecules are transported into the cell by diffusion or in the case of charged molecules by the electrophoretic force. After electroporation, the cells can be stained for transfection efficiency and viability analysis.

For successful electroporation with high efficiency and viability, it is important to properly choose the size and density of channels on the substrate such that each individual cell covers and seals multiple channels. If only partial sealing is achieved, significant electrical leakage may occur, and therefore a much higher input voltage would be required to trigger formation of nanopores in the cell membrane.[36,37] Applying high voltage is undesirable because it may damage cells by Joule heating or bubble formation. Therefore, the LEPD can be customized for different cells by selecting a substrate with the appropriate channel size and density to optimize transfection efficiency (see ESI,† Table S1). For this report, a polycarbonate (PC) substrate coated with poly-D-lysine (PDL) was used since it supported neuronal survival

and differentiation better than others including PDL-coated polyethylene or glass (see ESI†).

Device modeling

We utilized numerical modeling to assess the functionality of the LEPD and provide insight into the selection of substrate geometry to achieve optimal transfection efficiency. We explored two fundamental aspects of the LEPD: (1) quantitative prediction of the local electric field near a target cell and (2) time dependent molecular transport within the cell culture chamber. Accurate prediction of the local electric field created between a cell and substrate, for a given input voltage, is essential to determine the optimal range of applied voltages required to achieve a given transmembrane voltage. In addition, efficient delivery of molecules into cells relies on effective transport of the molecules into the cell culture chamber through the microchannels and the membrane channel connected to the cell on a timescale that allows for successful transfection.

Transmembrane electric potential drop. Unlike bulk electroporation where the entire cell membrane of each individual cell is exposed to a uniform electric field, the LEPD creates a localized electric field on the cell membrane area connected to the substrate channels. An accurate prediction of this local electric field is needed for selection of input voltages that results in successful electroporation. It is known that transfection does not occur when using an input voltage leading to a transmembrane voltage below a given threshold of 0.2–1 V.[43] Moreover, application of transmembrane voltages several times the threshold, may result in cell damage and low viability.[37] Therefore, selection of membrane diameters, D, and length, L, requires an electrostatic analysis.

To predict the distribution of the electric potential through a cell membrane, we used COMSOL Multiphysics to solve the partial differential equation $\nabla(\sigma\nabla V) = 0$ with appropriate geometric and boundary conditions. In the governing equation, V is the input electric potential and σ is the electrical conductivity.[44] The electric potential was applied at the bottom of the perforated substrate while the liquid at the top of a cylindrical microchamber is electrically grounded. These boundary conditions were used to model the two electrode configuration in the LEPD, one built-in on the glass slide and the other submerged into the cell culture chamber, respectively (Fig. 1). The cell membrane was modeled as a 5 nm layer enclosing a conductive media (cell cytosol). We assumed that the surfaces of the perforated substrate are electrically insulated. A cell with 10 μm diameter was positioned within a cylindrical well of 30 μm in radius and height. Further details including other key parameters and assumptions used in the analysis can be found elsewhere.[37]

We performed an electrostatic numerical simulation for a device with membrane channel length of 24 μm and diameters in the range of 200 nm to 2 μm (Fig. 2). The analysis predicts that an input voltage of 10 V results in a 0.06, 0.31, 0.56, and 1.3 V transmembrane potential drop for channel diameters of 200, 600, 1000, and 2000 nm, respectively. As expected, the required input voltage to achieve the threshold transmembrane voltage increases significantly with reduction in channel diameter (D). Since use of high voltages could result in substantial decrease in cell viability due to electric Joule heating or bubble formation, channel diameter must be carefully selected. Indeed, channel diameter is also controlled by the size of cells under study because it needs to be significantly smaller than the average cell diameter while in suspension prior to platting. Thus, although our analysis

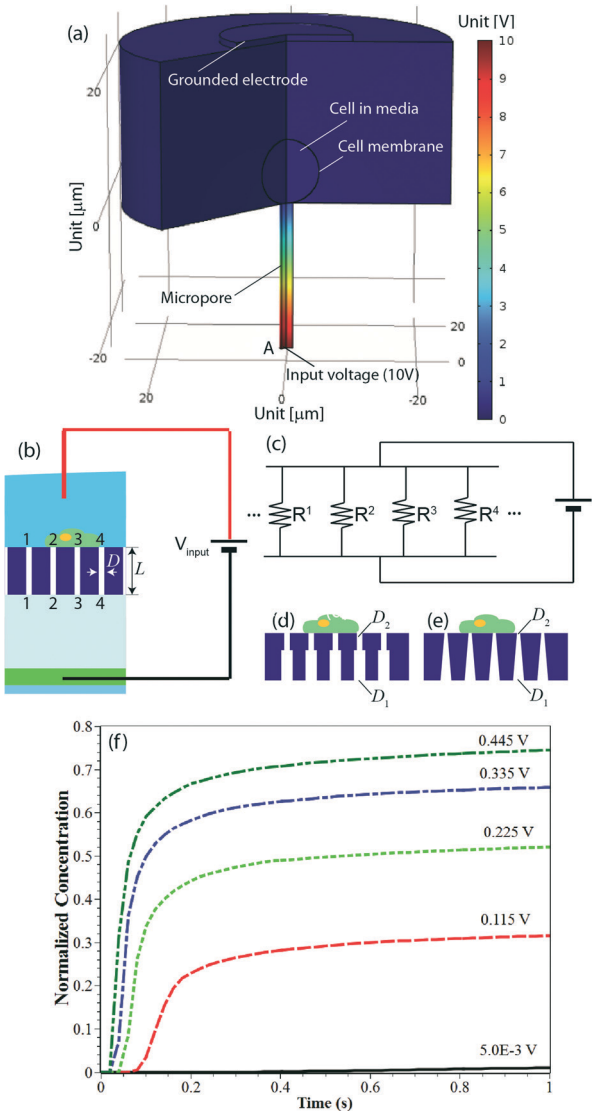

Fig. 2 (a)–(b) Numerical simulation of electric field in the LEPD. (b) Magnified view of area A in Fig. 1a showing substrate channels connected to a cell at the top and a fluidic microchannel at the bottom. (c) Lumped model for the electrical circuit of (b). Note that the potential drop through each substrate channel is independent from each other. (d) and (e) are examples of other possible microchannel geometries, bi-diameter and tapered channels, respectively. (f) Normalized molecular concentration at the interface between a cell and substrate channel as a function of time for various applied voltages.

gives general design criteria and guidelines for input voltages, the channel size needs to be optimized depending on cell size and type.

Note that the potential drop occurs along the channel, Fig. 2a; therefore, the cell is exposed only to an electric field that is localized on a small area of the cell membrane. This minimizes cell stress and increases viability.[37] Because the substrate channels are electrically connected in parallel, the potential drop through each one is independent (see Fig. 2b–c). Thus, our numerical results based on the single membrane channel are applicable to predict the transmembrane potential drop that occurs when a cell seals multiple channels on a perforated substrate. Furthermore, the simulation predicts that for D = 2 μm and an input voltage greater than 7.7 V, the transmembrane voltage drop becomes larger than the threshold voltage needed for electroporation.

Although the implementation of the LEPD in this manuscript utilized a perforated substrate with channels of uniform diameter, D, there are other design strategies that could tailor the electric field near a target cell for a given input voltage. For instance, channels with different cross section can be used, *e.g.*, bi-diameter or tapered channels as schematically represented in Fig. 2d–e, respectively. Alternatively, electrical resistance of a channel can be reduced by decreasing its length, L, decreasing in the input voltage required to achieve the threshold transmembrane potential drop. In practice, we found that manipulation of a perforated membrane becomes increasingly challenging when $L < 10$ μm.

Transport of molecules. Another feature of the LEPD that needs investigation is the molecular transport and molecular concentrations near a cell adhered to the substrate. We performed a numerical study in which two scenarios were considered: (a) pure diffusion due to a concentration gradient of the molecules within the substrate channel and (b) diffusion under the influence of an electrophoretic force. The latter is relevant because most biomolecules are charged, and upon exposure to the electrical field used for electrophoretic, transport will be a function of the electrophoretic force. In this calculation, we assume a constant molecular concentration at the bottom of the channel in the perforated substrate (denoted A in Fig. 2a).

(a) Pure diffusion case. First, we consider a scenario where transport of molecules through the membrane channel occurs *via* pure diffusion. The governing equation is: $\frac{\partial c_i}{\partial t} + \nabla\cdot\left(-D_i\nabla c_i\right) = s_i$, where c_i, D_i and s_i are the concentration, diffusion mobility, and source generation terms for the '*i*th' species,[45] respectively. The initial boundary value problem was numerically solved using channel dimensions of 2 μm in diameter and 24 μm in length. Our numerical analysis revealed that diffusion through the channel does not occur on a timescale relevant to high throughput biological experiments. For example, a normalized concentration (actual concentration normalized to the concentration in the circulation microchannel) of 10% is achieved in the vicinity of the cell within half an hour. Note that formation and recovery of nanopores in a cell membrane, during electroporation, occurs within a time scale of seconds.[46] The implication is that by just circulating a solution containing the molecules to be transfected in the microchannel, a waiting period of ~30–60 minutes would be required before transfection would occur by applying the electroporation pulses.

(b) Electrophoretic transport case. The concentration profiles of molecules, through the substrate channel, were analyzed as a function of electric field strength and time (Fig. 2f). The membrane channel was modeled as a cylindrical well (Fig. 2a) where the concentration profile under the influence of an electric field is $\frac{\partial c_i}{\partial t} + \nabla\cdot\left(-D_i\nabla c_i - z_i u_{\mathrm{m},i} F c_i \nabla V\right) = s_i$, where z_i is the ionic charge, $u_{\mathrm{m},i}$ is the electrophoretic mobility, F is the Faraday's constant, and V is the applied voltage,[45] respectively. For this analysis, we used a diffusion coefficient of 1.0×10^{-10} m^2 s^{-1} and an ionic mobility of 2.59×10^{-13} s mol kg^{-1}.[47] Note that the electrophoretic mobility of charged molecules is usually two orders of magnitude higher than the diffusive mobility.[47]

The results of the simulation are summarized in Fig. 2f for input voltages between 0.005 and 0.445 V. Relatively low input voltages were considered to examine the effect of electrophoretic force on molecular transport while avoiding formation of nanopores in the cell membrane. This result suggests that electrophoretic diffusion at low input voltage can be used to achieve the desired concentration of molecules near a cell before or after performing electroporation. A substantial concentration of molecules in the channel and near the cell membrane is predicted in <0.5 s for simulated applied voltages in excess of 0.1 V. For example, the normalized concentration in the cylindrical well reaches approximately 50% within 0.1 s at 0.445 V. Increasing concentrations are achieved more quickly by increasing input voltage. The key conclusion of this simulation is that input voltages in the range of 10–20 V, which correlate to potential drops at the cell membrane of 1.3–2.6 V, will result in molecular transport on a timescale that enables electroporation to be carried out immediately after loading the solution into the microchannels. This conclusion is qualitatively validated in the electroporation section where successful transfection was achieved when the electroporation pulses were applied immediately after loading the device.

Electroporation results

To validate the device design and evaluate the numerical predictions, demonstrate transfection of multiple types of molecules, and develop electroporation protocols, we first tested the LEPD using HeLa and HT1080 cell lines. Electroporation experiments were performed to determine optimal parameters of input voltage and pulse duration for high efficiency of transfection and cell viability. In addition, transfection of different molecular sizes and concentrations were investigated to ensure that transfection of a wide range of molecules, relevant to many biological applications, can be achieved.

Delivery of propidium iodide. First we demonstrated transfection of propidium iodide (PI), which is not permeable through the membrane of live cells despite its small size (~700 Da), into HeLa cells plated on the LEPD. Ten μl of a 3 : 1 (v/v) solution of phosphate buffered saline (PBS) and PI was loaded into each microchannel. Cells on three different devices were independently electroporated by applying an input voltage of 20 V at 200 Hz. Two 1 s input square wave signals (input duration) with a 1 s time interval (resting duration) between pulses were applied (see Fig. S4a†). These parameters were chosen based on previous studies of transfection using NFP-E, which is also a localized electroporation technique.[36,37] After electroporation, we flushed the device to remove the PBS/PI solution by circulating cell media through the microchannels, stained the cells with Calcein AM, and stored the device in an incubator for 20 min before imaging. Fluorescence images of the cells were collected in green and red channels as shown in Fig. 3. Approximately 95% of the cells on the three different devices show both red and green fluorescence, which indicates that the cells were successfully transfected (red due to PI) and alive (green due to Calcein AM). Thus, we conclude that the efficiency in delivering PI into HeLa cells using the LEPD was ~95% with similar viability.

Delivery of plasmids. Delivering large molecules like DNA into cells is important for many biological studies. Therefore, we demonstrated the capability of the LEPD for delivering a 2 MDa green fluorescent protein (GFP) plasmid into HeLa cells by following the same protocol used for transfection of PI. In addition, we examined the effect of key parameters such as (a) concentration of GFP plasmid, and (b) amplitude and duration of input voltage on transfection efficiency. For consistency, the same number of cells was plated on identical LEPDs and each electroporation experiment was performed within 1 hour in all devices. After electroporation, the devices were incubated overnight to allow time for cells to express GFP. Optical images were taken from each LEPD in the same order as electroporation was performed to minimize variation in time among devices.

(a) Effect of plasmid concentration. Transfection of GFP plasmid at concentrations of 0.01, 0.02, 0.1, and 1 μg μl^{-1} was performed using identical voltage input signals (two square wave pulses of 1 s with 1 s interval). Immediately after injecting 10 μl of the GFP plasmid solution into the microchannels, cells were electroporated at 10 and 20 V and then placed in an incubator for 24 h. After incubation, fluorescence images were collected to monitor GFP expression by the HeLa cells. As shown in Fig. 4a–b, GFP plasmid was successfully transfected into HeLa cells at low concentrations (0.01 and 0.02 μg μl^{-1}). This result shows that the LEPD can deliver molecules into cells using small volumes at low concentrations, which is a useful feature for the transfection of expensive molecules. Interestingly, the cells electroporated with the higher concentrations of GFP plasmid (0.1 μg μl^{-1} in Fig. 4c and 1 μg μl^{-1} in Fig. S3†) showed a lower transfection efficiency, *i.e.*, fewer cells expressed GFP, and those that did exhibited abnormal cell morphology (rounded shape). The reason for this observation will be investigated in future work, but may be due in part to a change in conductivity of the solution as the concentration of GFP plasmid was varied. The cell damage that correlated to high GFP intensity may be due to stress from over-dosage of GFP plasmid.

(b) Effect of input voltage parameters. To study the effect of input voltage amplitude on transfection efficiency, HeLa cells were electroporated on two separate LEPDs at 5 and

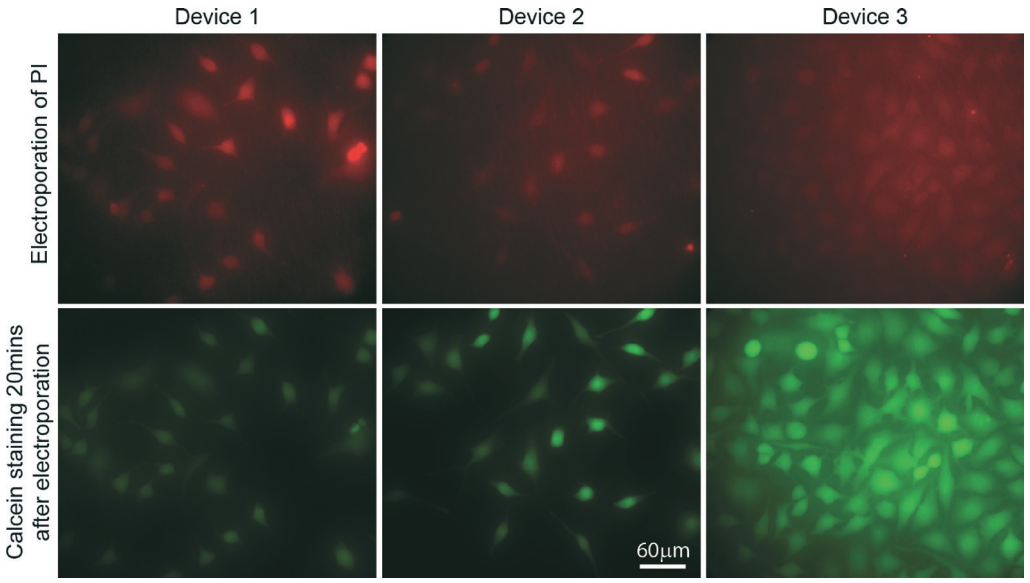

Fig. 3 Delivery of PI into HeLa cells. Top row shows images of electroporated cells in three different devices with efficiencies ranging from 92–100%. Bottom images show Calcein AM staining for quantification of cell viability.

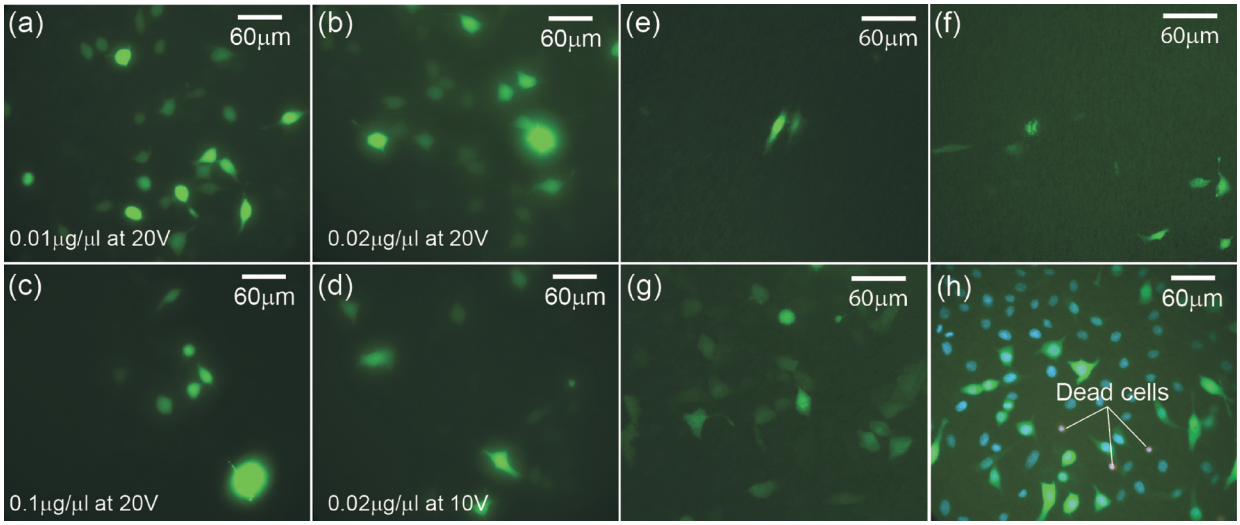

Fig. 4 Images of HeLa cells transfected with GFP plasmid using the LEPD. Results showing the effect of GFP plasmid concentration (a–c) and input voltage strength (d–g) on transfection efficiency are summarized. (e–f) show GFP expression after electroporation using 0.25, 0.5, and 0.75 s input voltage pulse duration, respectively. (h) is a merged image of green (GFP), blue (Hoechst), and red (PI) channels for viability assay (~97%).

10 V, respectively, with GFP plasmid at a concentration of 0.02 μg μl^{-1}. GFP expression was observed at 10 V (Fig. 4d), but not at 5 V. This is consistent with our numerical analysis, which revealed that far field voltage in excess of 7.7 V is needed to achieve the electroporation transmembrane voltage (see the device modeling section).

To explore the effect of input signal duration, HeLa cells were electroporated with a solution of 0.1 μg μl^{-1} GFP plasmid and several total pulse durations. We showed previously[37] that dosage of molecules delivered by electroporation increases with an increase in input pulse duration. Therefore, varying the number of pulses is expected to vary the dosage of GFP plasmid delivered into the cells. Fig. 4e–g displays the GFP expression from HeLa cells electroporated using one, two, or three 0.25 s square wave input signals, respectively, at 20 V and 200 Hz. The number of cells expressing GFP significantly increases with the increase in input pulse duration. Note that the concentration of GFP plasmid was the same for the experiments in Fig. 4c and e–g, yet the abnormal cell morphology is not observed for the latter experiments where the total pulse durations were 0.25, 0.50, and 0.75 s, respectively, compared to 2 s for the former.

Cell viability for all three pulse durations tested in Fig. 4e–g was examined by exposure to PI where cell death was found to be comparable to that on a control device without electroporation. For example, the merged image of green (GFP), blue (Hoechst 33342, Invitrogen), and red (PI) fluorescence shown in Fig. 4h revealed that only three HeLa cells were dead after electroporation with the longest total pulse duration (~97% viability). Further experimental studies revealed that transfection using the LEPD is gentle to cells such that the electroporated cells exhibit normal cell behavior including cell division. For example, HeLa cell division at 10 and 23 h after electroporation is shown in Fig. 5a and b, respectively.

(c) Validation in HT1080 cell line. Validation of the LEPD was further demonstrated by performing electroporation of GFP plasmid into HT1080 cells (Fig. 5c–d). Transfection efficiencies of up to 50% using a 30 V input signal at 200 Hz (0.25 s × 4 pulses) were achieved with GFP plasmid concentration of 0.1 μg μl^{-1}. Fig. 5c shows a merged image of green (GFP) and blue (Hoechst) channels after electroporation. Overall, these parametric studies showed that the LEPD is capable of delivering various molecules into immortalized

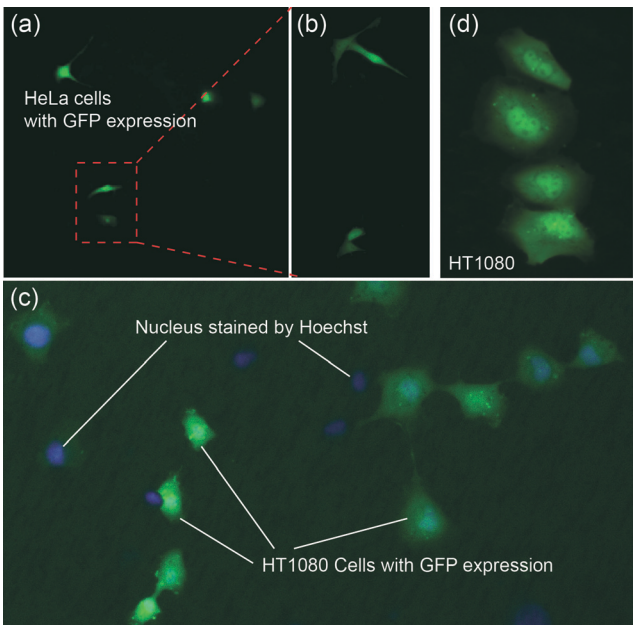

Fig. 5 Transfection of GFP plasmid into HeLa and HT1080 cells. (a) and (b) show fluorescence images of HeLa cells after electroporation and cell division, respectively. (c) and (d) show successful transfection of GFP plasmid into HT1080.

cell lines such as HeLa and HT1080 cells while maintaining high viability.

Transfection of postmitotic neurons

Unlike the robust cell lines used for the validation studies, neurons are much more sensitive primary cells; therefore, it is important to develop protocols specifically for primary cells. We focused on developing robust protocols for (1) long term cell culture on the LEPD and (2) their efficient transfection.

We started by examining long term cell culture on the device, which is necessary, for example, to support differentiation of neural stem cells and eliminate the need for suspending and/or re-plating mature cells. Following the protocols for on-chip cell culture described in the methods section, neural stem cells were plated on the LEPD and allowed to differentiate into neurons. For consistency, 12 identical LEPD devices were fabricated, plated with the same number of neural stem cells, and stored in the same incubator for 6 days. To monitor cell viability and morphology, the cells on two LEPDs were removed from the incubator every 24 hours and stained with Calcein AM over 6 days as shown in Fig. 6. We observed that the neural stem cells developed morphological features consistent with neurons-like cells including axon structures within 24 hours. Neuronal junctions were continuously formed between neighboring cells over time. We confirmed that the neural stem cells differentiated into neurons within 24 hours after plating on the LEPD using β-tubulin III, a biomarker for neurons as we will discuss further below.

Since the size of neural stem cells is much smaller than that of HeLa and HT1080 cells, a PC membrane with 600 nm diameter channels was used in the LEPDs. Our numerical analysis of the transmembrane electric potential drop revealed that the required input voltage to reach the critical transmembrane potential drop (~0.2–1 V) increases with reduction of pore size (~4.2 times when the diameter decreases from 2000 nm to 600 nm). Hence to achieve high transfection efficiency of DNA plasmids into neurons, we used higher input voltages (80–100 V). In addition, we found that application of square waves at such high input voltage may result in formation of bubbles. To resolve this issue, we reduced the pulse duration by using bi-level pulses (Fig. S4b†). Further details on the bi-level waves employed during transfection of neurons can be found in the ESI.†

Differentiated neural stem cells were electroporated using GFP plasmid at a concentration of 0.1 μg μl^{-1} in neuron media. After electroporation, the cells were incubated for 24 hours to allow time for GFP expression (Fig. 6a–c). To confirm that the cells on the LEPD were indeed neurons, β-tubulin III, a biomarker for neurons, was stained with Alexa Fluor 594 (Fig. 6d). A merged image combining red and blue channels, Fig. 6e, shows that all neural stem cells

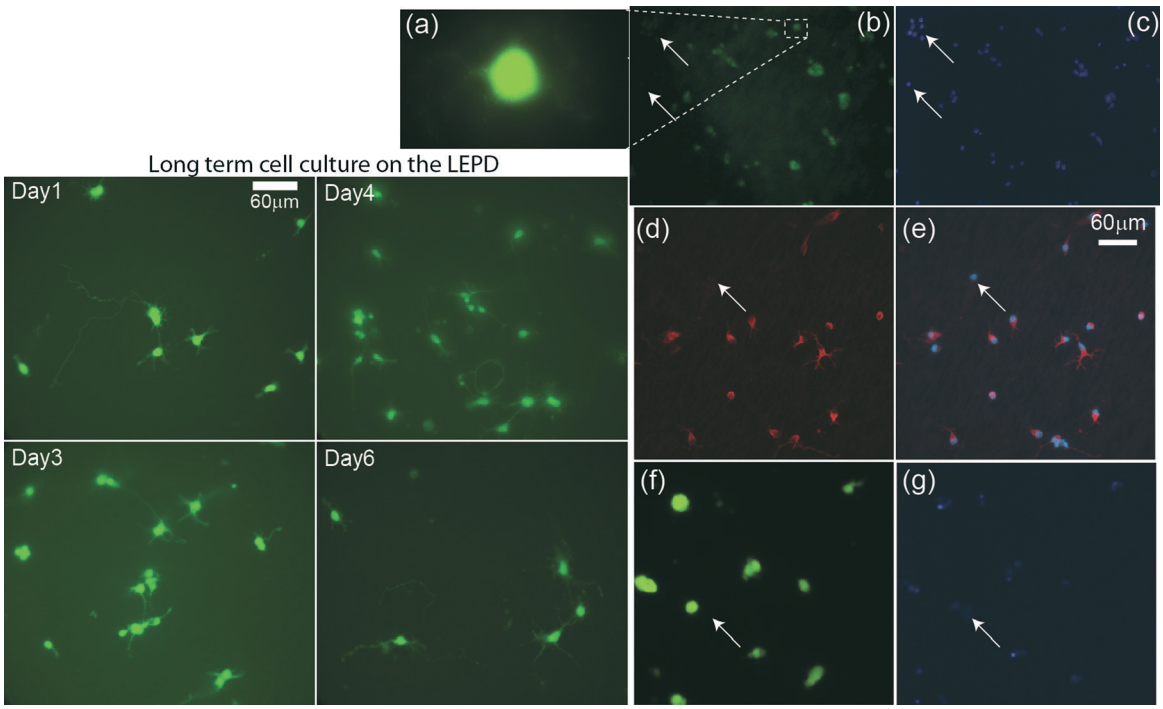

Fig. 6 Long term cell culture on the LEPD. Neural stem cells from 5 day old neurospheres were plated on the devices to monitor differentiation and viability of neural stem cells, using calcein AM staining, over a period of 6 days. Electroporation of postmitotic neurons using LEPD. The green fluorescent images in (a)–(b), taken 24 hours after electroporation of GFP plasmid, indicate successful transfection of neurons. The arrows in (b) and (c) indicate neurons without GFP expression. (d) To confirm that the neuron-like cells on the LEPD are indeed neurons, a biomaker for neurons (β-tubulin III) was tagged to red fluorescent dye. (e) is a merged image between red and blue (Hoechst) channels. For viability assay, neurons were stained using Calcein AM (f) and Hoechst (g), respectively. The arrows in (d) and (e) indicate a cell without β-tubulin.

in the field of view, except the one indicated with the arrow, were fully differentiated into neurons. For the viability test, electroporated neurons on the LEPD were stained with Calcein AM and Hoechst, 48 hours after electroporation, as shown in Fig. 6f and g, respectively. Cells with green fluorescence, either due to GFP or Calcein, correspond to live cells within the field of view, >90% of the cells remain viable. This result reveals that the LEPD produced high viability after electroporation, indicating that localized electroporation, at the substrate channel-cell membrane interface, is indeed gentle to cells.

Experimental

Microdevice fabrication and assembly

The device microfabrication steps are summarized in Fig. S5.† Microelectrodes were fabricated on glass cover slides (Nova) using a lithography-based microfabrication technique. Thin films of chromium (adhesion layer) and gold were deposited by thermal evaporation, and photoresist (PR) was spin-coated on the cover slide. The PR layer was then exposed to UV light and patterned using a developer. The metallic thin films were etched by wet etching to create microelectrodes. The PR layer was then removed by acetone. Finally, the cover slide with built-in electrodes was rinsed with DI water.

For fabrication of the PDMS layers, we made a PR mold (SU8) on a wafer using a lithography-based microfabrication technique. All PDMS layers and cover slides have alignment marks for ease of assembly using an optical microscope. For permanent bonding of PDMS to PDMS and PDMS to glass surfaces, the surfaces to be bonded were treated by oxygen plasma, optically aligned, and thermally annealed in an oven at 75 °C for 6 hours. Likewise, an optical microscope was used to assemble the polycarbonate (PC) membrane (AR Brown-US) between PDMS layers.[48] The dimensions of the PC membranes are given in the ESI.†

Electroporation and detection protocols

Cells in suspension were circulated and plated on the devices. The device was stored in an incubator at 37 °C and 5% CO_2 for 24 hours in preparation for electroporation. For the HeLa and HT1080 electroporation experiments, 10 μl of a 3 : 1 (v/v) solution of PBS and PI (eBioscience) or GFP plasmid at concentrations of 0.01, 0.02, 0.1, and 1 μg μl^{-1}, in incomplete Dulbecco's Modified Eagle Medium (DMEM, Sigma) was fed to the cell culture chamber. Immediately after loading the solution into the microchannels, the LEPD containing plated cells was connected to a power source and then the electrical input signals applied for electroporation.

The external electrical signal was generated by a pulse generator (DS345, Stanford Research Systems), amplified by a voltage amplifier (OPA445, Texas Instruments), and monitored using an oscilloscope (9384L, LeCroy). Before applying voltage, we confirmed the electrical connection by measuring resistance between the two electrodes, which was typically in the range of 5–10 kΩ. The desired electrical input was then applied to trigger formation of nanopores on the cell membranes to achieve transfection. After electroporation, the LEPDs were kept in an incubator. For any additional staining of cells on the LEPD, the solutions were fed through the microchannels, the device was kept in an incubator during cell staining, and the solutions were flushed by circulating cell media. All optical images were taken using an inverted fluorescence microscope (Eclipse Ti-U, Nikon) equipped with a CCD camera (Neo sCMOS, Andor).

Cell culture and staining

We obtained HeLa cells from the American Type Culture Collection (ATCC #CCL-2) and HT1080 cells from the Tsourkas Lab at University of Pennsylvania, respectively. We cultured both cell lines in Dulbecco's Modified Eagle Medium (SIGMA) with L-glutamine and phenol red as pH indicator, supplemented with 10% FBS (SIGMA) and 1X penicillin/streptomycin (Sigma). For transfection efficiency and viability, three different staining solutions, *i.e.*, Hoechst, PI and Calcein AM, were used. To evaluate the total number of cells on the LEPD, cell nuclei were stained by Hoechst 33342 (Invitrogen). For cell viability testing after long term on-chip cell culture and electroporation, PI (eBioscience) and Calcein AM (Life Technology), the most commonly used protocols for viability assay, were used to stain dead and live cells, respectively.

Neurons were differentiated from neurospheres obtained from the Kessler laboratory at Northwestern University. To isolate neural progenitor cells (NPC) and differentiate neurons, we followed the protocol given in ref. 49 with slight modifications. E13 embryos from CD1 mice (Charles River, Wilmington, MA) were dissected and the ganglionic eminences isolated and grown in serum-free medium (SFM) with human recombinant epidermal growth factor (FGF, 20 ng ml^{-1}, Biosource) for 5 days until neurospheres developed. After five days, neurospheres were passaged with 0.25% trypsin (Life Technologies) for 5 min, followed by the addition of soybean trypsin inhibitor (Life Technologies) and centrifugation for 5 min. After repeated pipetting to dissociate the neurospheres into single NPCs, the cells were cultured for an additional 3–4 days in SFM. For neuron differentiation, media containing SFM and 1 ng ml^{-1} FGF (human recombinant, Biosource) was used. Dissociated neurospheres in 200 μl of media were plated at a density of 50 000 cells ml^{-1} on each LEPD. The device and glass slides were coated with poly-D-Lysine (PDL, Sigma). For the PDL coating, LEPD and glass slides were kept overnight in PDL solution at the concentration of 20 μg ml^{-1} at 4 °C. During differentiation, the LEPD with the dissociated neurospheres were kept in an incubator for 1–6 days.

To monitor neuron differentiation, we stained for β-tubulin III after fixing the neurons plated on the LEPD with 100% methanol. After gently rinsing using PBS with 5% FBS,

the primary antibody that binds to β-tubulin III, monoclonal *anti*-β-tubulin III antibody (Sigma), was applied to the cells. After incubating the cells for 1 hour at 4 °C, the device was thoroughly rinsed with PBS and incubated with secondary antibodies conjugated to Alexa Fluor 594 (Molecular Probes) in the dark at 4 °C for 1 hour. Then the device was rinsed with PBS and fluorescent images were taken.

Conclusion

Toward development of an efficient tool for on-chip cell culture, differentiation, and transfection of primary cells, we have designed a microfluidic device capable of repeated, temporal delivery of molecules into a population of cells. We validated the design and electroporation protocols using HeLa and HT1080 cell lines and then demonstrated differentiation and transfection of postmitotic neurons. Utilizing unique advantages of the LEPD configuration, localized electroporation was achieved that offers unprecedented capabilities such as (1) transfection of various molecules into primary cells, *e.g.*, mouse neurons *in vitro* with temporal control, (2) maintenance of consistent pH levels or osmolarity by continuous media circulation, (3) application of a focused electric field to a small portion of the cell membrane to minimize stress, and (4) wide applicability of the method to various cell types. In addition, the devices are cost effective and simple to use.

The LEPD for localized electroporation shows great potential for time-dependent cell biology, gene expression, and protein interaction studies. The small size of the LEPD allows for its integration with an inverted microscope with enclosure for environmental control of temperature, humidity, and CO_2. This feature enables continuous optical monitoring of cells for long term study of the same selected cells over time and the ability to perform multiple transfections. By combining this unique feature with automated and precise control of flow through microchannels, long term cell culture and transfection of sensitive primary cells are possible without exposing the cells to non-sterile or uncontrolled environments.

Non-destructive longitudinal monitoring of cells is a much needed capability for study of cellular pathways and regulatory networks. We envision possibilities to expand the capabilities of the LEPD for single-cell biochemical profiling, using reverse electroporation sampling, and electrophysiology, by coupling various electrical and optical sensing modalities either integrated to the device or accessing cells from the top of the LEPD, to directly study the dynamic responses of cells with minimal perturbation to their differentiation or maturation.

Acknowledgements

This work was supported by the National Science Foundation under award IIP-1330151 and the National Institutes of Health under award 1R41GM101833. We acknowledge contributions made by H. Zhao on the fabrication of the device. We thank Professor Andrew Tsourkas of the Department of Bioengineering Chemistry at University of Pennsylvania for providing HT1080 cells.

Notes and references

1 G. M. Schratt, F. Tuebing, E. A. Nigh, C. G. Kane, M. E. Sabatini, M. Kiebler and M. E. Greenberg, *Nature*, 2006, **439**, 283–289.
2 B. N. G. Giepmans, S. R. Adams, M. H. Ellisman and R. Y. Tsien, *Science*, 2006, **312**, 217–224.
3 T. H. Ward and J. Lippincott-Schwartz, *Methods Biochem. Anal.*, 2006, **47**, 305–337.
4 R. Dahm, M. Zeitelhofer, B. Gotze, M. A. Kiebler and P. Macchi, *Methods Cell Biol.*, 2008, **85**, 293–327.
5 S. Huttelmaier, D. Zenklusen, M. Lederer, J. Dictenberg, M. Lorenz, X. H. Meng, G. J. Bassell, J. Condeelis and R. H. Singer, *Nature*, 2005, **438**, 512–515.
6 N. Heim, O. Garaschuk, M. W. Friedrich, M. Mank, R. I. Milos, Y. Kovalchuk, A. Konnerth and O. Griesbeck, *Nat. Methods*, 2007, **4**, 127–129.
7 O. Gresch, F. B. Engel, D. Nesic, T. T. Tran, H. M. England, E. S. Hickman, I. Korner, L. Gan, S. Chen, S. Castro-Obregon, R. Hammermann, J. Wolf, H. Muller-Hartmann, M. Nix, G. Siebenkotten, G. Kraus and K. Lun, *Methods*, 2004, **33**, 151–163.
8 S. N. Kalburgi, N. N. Khan and S. J. Gray, *Discov. Med.*, 2013, **81**, 111–119.
9 M. Barkats, A. Bilang-Bleuel, M. H. Buc-Caron, M. N. Castel-Barthe, O. Corti, F. Finiels, P. Horellou, F. Revah, O. Sabate and J. Mallet, *Prog. Neurobiol.*, 1998, **55**, 333–341.
10 H. Buning, L. Perabo, O. Coutelle, S. Quadt-Humme and M. Hallek, *J. Gene Med.*, 2008, **10**, 717–733.
11 M. Simonato, R. Manservigi, P. Marconi and J. Glorioso, *Trends Neurosci.*, 2000, **23**, 183–190.
12 Y. Zhang and L. C. Yu, *Bioessays*, 2008, **30**, 606–610.
13 C. Lappe-Siefke, C. Maas and M. Kneussel, *J. Neurosci. Methods*, 2008, **175**, 88–95.
14 X. Xie, A. M. Xu, S. Leal-Ortiz, Y. H. Cao, C. C. Garner and N. A. Melosh, *ACS Nano*, 2013, **7**, 4351–4358.
15 F. Yamauchi, K. Kato and H. Iwata, *Nucleic Acids Res.*, 2004, 32.
16 T. Saito, *Nat. Protoc.*, 2006, **1**, 1552–1558.
17 P. G. Leclere, A. Panjwani, R. Docherty, M. Berry, J. Pizzey and D. A. Tonge, *J. Neurosci. Methods*, 2005, **142**, 137–143.
18 M. N. Teruel, T. A. Blanpied, K. Shen, G. J. Augustine and T. Meyer, *J. Neurosci. Methods*, 1999, **93**, 37–48.
19 S. D. Dib-Hajj, J. S. Choi, L. J. Macala, L. Tyrrell, J. A. Black, T. R. Cummins and S. G. Waxman, *Nat. Protoc.*, 2009, **4**, 1118–1127.
20 Y. H. Zhan, Z. N. Cao, N. Bao, J. B. Li, J. Wang, T. Geng, H. Lin and C. Lu, *J. Controlled Release*, 2012, **160**, 570–576.
21 T. Geng and C. Lu, *Lab Chip*, 2013, **13**, 3803–3821.

22 A. Valero, J. N. Post, J. W. van Nieuwkasteele, P. M. ter Braak, W. Kruijer and A. van den Berg, *Lab Chip*, 2008, **8**, 62–67.
23 A. Valero, F. Merino, F. Wolbers, R. Luttge, I. Vermes, H. Andersson and A. van den Berg, *Lab Chip*, 2005, **5**, 49–55.
24 M. B. Fox, D. C. Esveld, A. Valero, R. Luttge, H. C. Mastwijk, P. V. Bartels, A. van den Berg and R. M. Boom, *Anal. Bioanal. Chem.*, 2006, **385**, 474–485.
25 B. Judkewitz, M. Rizzi, K. Kitamura and M. Hausser, *Nat. Protoc.*, 2009, **4**, 862–869.
26 J. Rathenberg, T. Nevian and V. Witzemann, *J. Neurosci. Methods*, 2003, **126**, 91–98.
27 K. Kitamura, B. Judkewitz, M. Kano, W. Denk and M. Hausser, *Nat. Methods*, 2008, **5**, 61–67.
28 D. Karra and R. Dahm, *J. Neurosci.*, 2010, **30**, 6171–6177.
29 J. J. VanDersarl, A. M. Xu and N. A. Melosh, *Nano Lett.*, 2012, **12**, 3881–3886.
30 A. K. Shalek, J. T. Robinson, E. S. Karp, J. S. Lee, D. R. Ahn, M. H. Yoon, A. Sutton, M. Jorgolli, R. S. Gertner, T. S. Gujral, G. MacBeath, E. G. Yang and H. Park, *Proc. Natl. Acad. Sci. U. S. A.*, 2010, **107**, 1870–1875.
31 S. J. Qi, C. Q. Yi, S. L. Ji, C. C. Fong and M. S. Yang, *ACS Appl. Mater. Interfaces*, 2009, **1**, 30–34.
32 M. van Engeland, L. J. W. Nieland, F. C. S. Ramaekers, B. Schutte and C. P. M. Reutelingsperger, *Cytometry*, 1998, **31**, 1–9.
33 J. Gehl, *Acta Physiol. Scand.*, 2003, **177**, 437–447.
34 W. Krassowska and P. D. Filev, *Biophys. J.*, 2007, **92**, 404–417.
35 M. Zeitelhofer, J. P. Vessey, Y. Xie, F. Tübing, S. Thomas, M. Kiebler and R. Dahm, *Nat. Protoc.*, 2007, **2**, 1692–1704.
36 W. Kang, R. L. McNaughton, F. Yavari, M. Minary-Jolandan, A. Safi and H. D. Espinosa, *J. Lab. Autom.*, 2014, **19**, 100–109.
37 W. Kang, F. Yavari, M. Minary-Jolandan, J. P. Giraldo-Vela, A. Safi, R. L. McNaughton, V. Parpoil and H. D. Espinosa, *Nano Lett.*, 2013, **13**, 2448–2457.
38 Y. Chisti, *Crit. Rev. Biotechnol.*, 2001, **21**, 67–110.
39 G. Kretzmer and K. Schugerl, *Appl. Microbiol. Biotechnol.*, 1991, **34**, 613–616.
40 A. Ludwig, G. Kretzmer and K. Schugerl, *Enzyme Microb. Technol.*, 1992, **14**, 209–213.
41 E. D. Goluch, J. M. Nam, D. G. Georganopoulou, T. N. Chiesl, K. A. Shaikh, K. S. Ryu, A. E. Barron, C. A. Mirkin and C. Liu, *Lab Chip*, 2006, **6**, 1293–1299.
42 R. Gomez-Sjoberg, A. A. Leyrat, D. M. Pirone, C. S. Chen and S. R. Quake, *Anal. Chem.*, 2007, **79**, 8557–8563.
43 M. Y. Wang, O. Orwar, J. Olofsson and S. G. Weber, *Anal. Bioanal. Chem.*, 2010, **397**, 3235–3248.
44 A. Agarwal, I. Zudans, E. A. Weber, J. Olofsson, O. Orwar and S. G. Weber, *Anal. Chem.*, 2007, **79**, 3589–3596.
45 J. H. Masliyah and S. Bhattacharjee, *Electrokinetic and colloid transport phenomena*, Wiley-Interscience, Hoboken, N.J., 2006.
46 C. Chen, S. W. Smye, M. P. Robinson and J. A. Evans, *Med. Biol. Eng. Comput.*, 2006, **44**, 5–14.
47 N. C. Stellwagen, C. Gelfi and P. G. Righetti, *Biopolymers*, 1997, **42**, 687–703.
48 J. J. VanDersarl, A. M. Xu and N. A. Melosh, *Lab Chip*, 2011, **11**, 3057–3063.
49 M. A. Bonaguidi, T. McGuire, M. Hu, L. X. Kan, J. Samanta and J. A. Kessler, *Development*, 2005, **132**, 5503–5514.